IAC-19,C4,6,3,x49922

## Inductive Plasma Thruster (IPT) design for an Atmosphere-Breathing Electric Propulsion System (ABEP)

**F. Romano[aa*], G. Herdrich[aa], P. C.E. Roberts[a], Y.-A. Chan[aa], C. Traub[aa], S. Fasoulas[aa], K. Smith[a], S. Edmondson[a], S. Haigh[a], N. Crisp[a], V. T. Abrao Oiko[a], R. Lyons[a], S. D. Worrall[a], S. Livadiotti[a], C. Huyton[a], L. Sinpetru[a], R. Outlaw[a], J. Becedas[b], R. M. Dominguez[b], D. González[b], V. Hanessian[c], A. Mølgaard[c], J. Nielsen[c], M. Bisgaard[c], D. Garcia-Almiñana[d], S. Rodriguez-Donaire[d], M. Sureda[d], D. Kataria[e], R. Villain[f], J. Santiago Perez[f], A. Conte[f], B. Belkouchi[f], A. Schwalber[g], B. Heißerer[g], M. Magarotto[h], D. Pavarin[i]**

[aa] *Institute of Space Systems (IRS), University of Stuttgart, Pfaffenwaldring 29, 70569, Germany*

[a] *The University of Manchester, Manchester,* George Begg Building, Sackville Street, Manchester, M13 9PL, UK.

[b] *Elecnor Deimos Satellite Systems,* Calle Francia 9, 13500 Puertollano, Spain

[c] *GomSpace AS*, Langagervej 6, 9220 Aalborg East, Denmark

[d] *UPC-BarcelonaTECH,* Carrer de Colom 11, 08222 Terrassa, Barcelona, Spain

[e] *Mullard Space Science Laboratory (UCL),* Holmbury St. Mary, Dorking, RH5 6NT, United Kingdom

[f] *Euroconsult,* 86 Boulevard de Sébastopol, 75003 Paris, France

[g] *concentris research management gmbh,* Ludwigstraße 4, D-82256 Fürstenfeldbruck, Germany

[h] *Center of Studies and Activities for Space "Giuseppe Colombo" - CISAS,* Via Venezia 15, 3513 Padua, Italy

[i] *Università degli Studi di Padova, Industrial Engineering Department DII,* Via Gradenigo 6/a, 3513 Padua, Italy

## ABSTRACT

Challenging space missions include those at very low altitudes, where the atmosphere is source of aerodynamic drag on the spacecraft, therefore an efficient propulsion system is required to extend the mission lifetime. One solution is Atmosphere-Breathing Electric Propulsion (ABEP). It collects atmospheric particles to use as propellant for an electric thruster. This would minimize the requirement of limited propellant availability. The system could be applied to any planet with atmosphere, enabling new mission at these altitude ranges for continuous orbiting. Challenging is also the presence of reactive chemical species, such as atomic oxygen in Earth orbit. Such components are erosion source of (not only) propulsion system components, i.e. acceleration grids, electrodes, and discharge channels of conventional EP systems (RIT and HET). IRS is developing within the DISCOVERER project an intake and a thruster for an ABEP system. This paper deals with the design and first operation of the inductive plasma thruster (IPT) developed at IRS. The paper describes its design aided by numerical tools such as HELIC and ADAMANT. Such a device is based on RF electrodeless discharge aided by externally applied static magnetic field. The IPT is composed by a movable injector, to variate the discharge channel length, and a movable electromagnet to variate position and intensity of the magnetic field. By changing these parameters along with a novel antenna design for electric propulsion, the aim is to achieve the highest efficiency for the ionization stage by enabling the formation of helicon-based discharge. Finally, the designed IPT is presented and the feature of the birdcage antenna highlighted.

Keywords: ABEP, IPT, VLEO, HELICON, BIRDCAGE, RAM-EP

**Acronyms/Abbreviations**
ABEP: Atmosphere-Breathing Electric Propulsion
IPT: Inductive Plasma Thruster
VLEO: Very Low Earth Orbit
S/C: Spacecraft

## INTRODUCTION

The Inductive Plasma Thruster (IPT) is designed within the EU H2020 DISCOVERER project, that aims to redesign very-low Earth orbit (VLEO <400 km) platforms by researching on low drag materials, attitude control by aerodynamics, and with the developing an Atmosphere-Breathing Electric Propulsion system (ABEP) see Figure 1.
Orbiting in VLEO can open a new range of space missions, however, the mission lifetime is limited due to aerodynamic drag. To have longer missions, the spacecraft requires a propulsion system that compensates the drag in an efficient matter. An ABEP system is hereby proposed as a solution. Such system collects the atmospheric particles in VLEO by an intake, that feeds an electric thruster, which ionizes and accelerates them for thrust generation. An ABEP system theoretically removes the lifetime limits due to drag and due to the available propellant on-board. The propulsion system must operate with $N_2$ and O as propellant in Earth orbit. An ABEP system is not only

applicable to Earth orbit, but to any planet with atmosphere given that enough electric power is provided. Within DISCOVERER an RF-based contact-less thruster, the IPT, is developed, so to remove any issue of any component in contact with the plasma that would erode rapidly due to the use of atomic oxygen O as propellant. Such thruster is, moreover, neutralizer free as the exhaust plume is already neutral.

## ATMOSPHERE-BREATHING ELECTRIC PROPULSION

In an Atmosphere-Breathing Electric Propulsion (ABEP) system, an intake collects the residual atmosphere of a celestial body, and use it to feed an electric thruster. This ionizes and accelerates the atmospheric particles to produce thrust. In this particular case an inductive plasma thruster is used, see Figure 1.
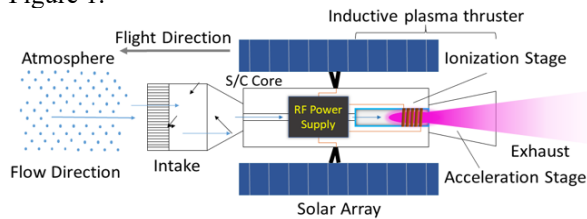


*Figure 1 ABEP Concept [1]*

## INDUCTIVE PLASMA THRUSTER DESIGN

The starting point of the IPT has been the heritage of IRS of inductive plasma generators (IPG). Major upgrades have been performed for the small-scale IPG6-S in the last years [2], [3]. Recent test campaigns have shown a large increase of power absorption by applying an external magnetic field to the source [4] and hence confirmed the feasibility of an improved plasma source that makes use of applied fields, especially as it possibly can trigger the helicon wave-mode, to operate the same magnetic field for an EM-based acceleration stage. The requirements within DISCOVERER are of an RF contact-less plasma thruster operated with variable mixtures of $N_2$ and O as propellant with $P_{in}$ < 5 kW. To cope with the chemically aggressive atomic oxygen, one of the main species in VLEO, IPT must avoid any direct contact with the plasma, so to reduce erosion to a minimum extent. In conventional EP systems, such as gridded ion thrusters and Hall-effect thruster, erosion of grids and discharge channels, will reduce thruster's performance over time very rapidly [5], [6]. The IPT, generates a neutral plasma plume that does not require a neutralizer, is another challenging device to design for atmospheric propellant operation [7], [8]. The first

version of the IPT is a laboratory model designed for maximum (technical) flexibility and passive cooling, to allow easy modifications for optimization purposes. Following the design of mechanical and vacuum interfaces [9], the crucial element of the IPT design is the antenna which will be described in the following section.

## ANTENNA DESIGN

According to results from HELIC and ADAMANT [4] a frequency higher than 27.12 MHz is preferable, as leading to easier ignition and better power absorption at higher plasma densities when associated with an externally applied DC magnetic field [10], [11]. Finally, an RF-Generator and an auto-matching network operating at 40.68 MHz for a power up to 4 kW has been acquired. The first antenna approach has been a coil-type antenna, the simulations have shown to provide better performance than a half-helical antenna, more commonly used in helicon plasma sources [4]. The discharge channel has been selected with 37 mm inner diameter (same as IPG6-S), with a variable number of turns coil antenna. Many coil antenna configuration, with different number of turns and plasma radii have been evaluated by using both HELIC [12], [13], and ADAMANT [14] tools. An RF-based plasma source can be modelled as a transformer, where the plasma is a resistance in the circuit. According to Chen [15], the plasma resistance $R_P$ must be high, at least higher than the circuit resistance $R_c$ so to maximize power absorption at the antenna, rather than in the circuitry. Finally, antenna and plasma have to be rather modelled as an equivalent impedance $Z$, with both real (resistance $R$) and imaginary (reactance $X$) components. In particular, the reactance $X$, is directly proportional to the applied frequency and has to be brought to zero, to minimize power reflection. The acquired power supply operating at $f$=40.68 MHz introduces an "a priori" higher reactance to the RF circuit that needs to be compensated. ADAMANT, compared to HELIC, gives as output the impedance $Z$, of the antenna plus the plasma, see Eq. (1).

$$\vec{Z} = \vec{R} + j\vec{X}$$
$$X = X_L + X_C = 2\pi f L + \left(-\frac{1}{2\pi f C}\right)$$

**(1)**

The numerical results for various plasma densities, magnetic fields, and coil antennas configurations, always resulted in a very high reactance $X$. Moreover, not only the antenna is to be considered for the thruster design, but the system at the whole, including the RF generator, its matching network, connectors, and connecting cables [16]. In an RF circuit, the power

transfer from a source (RF generator) to its load (antenna and plasma) is maximized only if the load's impedance $Z_L$ is matched to that of the source $Z_S$. RF generators standards is $Z_s=50 + j0\ \Omega$ purely resistive output. The matching network is introduced to create a resonant circuit with the load that is dynamically matched to $Z_S$ by a system of variable inductors and capacitors. This works mainly as protection for the RF generator, but it does not improve the load itself. Therefore, an optimum design of the antenna is required to maximize the power transfer from source to load. Plasma is finally a variable impedance that implies the need of a dynamic tuning control. An accurate selection of cabling, connectors and finally the antenna has been performed, the schematics is shown in Figure 2.
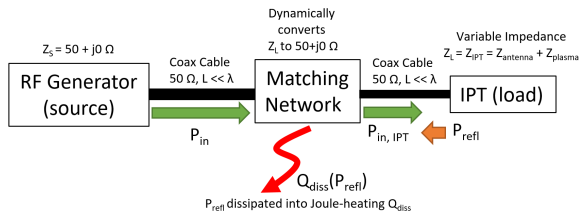


*Figure 2 Simplified IPT RF circuit* [17].

### THE BIRDCAGE ANTENNA

The seek of RF circuit optimization lead to the birdcage antenna. Such device has been developed in Magnetic Resonance Imaging (MRI) [18] and provides the very homogeneous magnetic required by the application. Birdcage antennas operate on the principle that a sinusoidal current distribution over a cylindrical surface will induce a homogeneous transversal magnetic field within the cylindrical volume itself. Such antennas are made by two end-rings, connected by equally spaced legs. The legs and/or the end-rings have capacitors in between to adjust the resonance frequency to the one required. Birdcage antennas can be designed as low-pass, high-pass, or band-pass frequency response depending on capacitor locations, see Figure *3*.
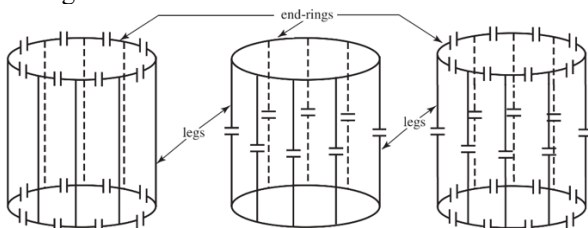


*Figure 3 Birdcage Antenna: high-pass (left), low-pass (middle), band-pass (right) (adapted from* [19]*).*

By operating birdcage antennas at one of their resonance frequencies, *X* is zero and its impedance *Z* is purely real. In this way the load is already partially

matched and only the resistance needs further matching. Moreover, at such resonance condition, the electromagnetic (EM) fields are perpendicular to each other and homogeneous within the cross section of the discharge channel. Depending on the feeding such fields are linearly or circularly polarized. At EPFL helicon plasma is generated for fusion research by birdcage antennas operating at 13.56 MHz for RF powers up to 10 kW [20]–[22]. Moreover, an older study from Guittienne directly investigated the use of birdcage antennas for an helicon based thruster [23].

Each antenna has $k = N/2$ resonant modes. The current distribution along the antenna follows the law described in Eq. (*2*), where $I_{jk}$ is the normalized current at the *j*-th loop for the *k* mode of a birdcage antenna with *N* legs.

$$I_{jk} = \begin{cases} cos\left(\dfrac{2\pi jk}{N}\right), & k = 0,1,2,\dots,N/2 \\ sin\left(\dfrac{2\pi jk}{N}\right), & k = 1,2,\dots,\left(\dfrac{N}{2}-1\right) \end{cases}$$

(2)

Therefore, the more legs, the more the current distribution matches a sinusoidal curve, see Figure 4.
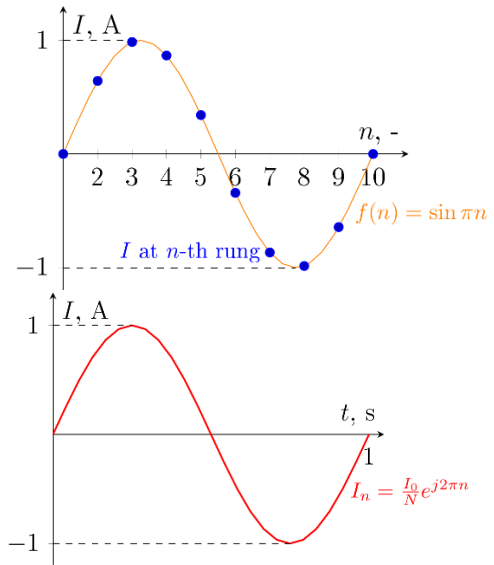


*Figure 4 Current distribution along a 10-leg birdcage at a given time (top), current amplitude over time on a single leg (bottom)* [17].

Birdcage antennas are modeled by self and mutual inductances of legs and end-rings $L_{Leg}$ and $L_{ER}$, plus the applied capacitors of capacitance *C*. Resonance frequencies for the high pass design are given in Eq. (*3*). The high pass design has one resonance mode more $(k = 0)$ at the highest frequency called anti-resonant AR.

$$\omega_{k_{HP}} = \left[ C \left( L_{ER} + 2\,L_{Leg}\,\sin^2\frac{\pi k}{N} \right) \right]^{-\frac{1}{2}}$$

$$(k = 0,1,2,\dots,N/2)$$

**(3)**

Only one resonant mode at $k = 1$ presents the required EM fields configuration.

In terms of EM fields, the magnetic field created by the birdcage is $\vec{B}_1$ along $y$, the respective electric field $\vec{E}_1$ is perpendicular to $\vec{B}_1$, along $x$, see Figure 5. Since $\vec{B}_1$ is linearly polarized, its direction will switch along $y$ on each cycle, and so will $\vec{E}_1$ along $x$. An additional external DC magnetic field is provided along the $z$ axis $\vec{B}_0$ for aiding formation of helicon waves.
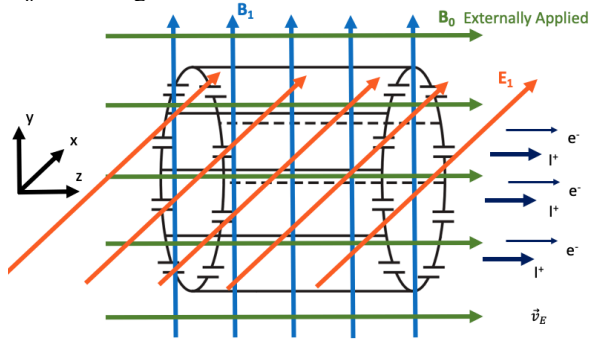


*Figure 5 Birdcage EM fields B₁, E₁, externally applied magnetic field B₀.*

The resulting EM fields, which still excludes of the plasma, provides a drift (exhaust) velocity $\vec{v}_E = \vec{E} \times \vec{B}$. This is imparted to ions and electrons to the same direction along $z$. This provide already some thrust while producing a quasi-neutral plasma exhaust that will not required the implementation of a neutralizer, see Eq. (4). Such results supports the use of birdcage antenna for a contact-less plasma thruster application without needing a neutralizer.

$$\vec{v}_E = \frac{1}{\vec{B}^2} \begin{Vmatrix} \hat{x} & \hat{y} & \hat{z} \\ E_1 & 0 & 0 \\ 0 & B_1 & B_0 \end{Vmatrix} = \frac{1}{B_0{}^2 + B_1{}^2} \begin{Bmatrix} 0 \\ -E_1 B_0 \\ E_1 B_1 \end{Bmatrix}$$

**(4)**

## IPT DESIGN WITH A BIRDCAGE ANTENNA

The IPT main components are: propellant injector, discharge channel, birdcage antenna, shield, electromagnet and the support structure, see Figure 6. The injector is movable along the symmetry axis $z$, as well as the external electromagnet, that can produce a magnetic field up to 70 mT with 15 A DC current. At such a current more than 30 min operation are possible without overheating, to allow plasma diagnostic measurements.

A birdcage with 8 legs in a high pass design has been chosen. It is designed to resonate at 40.68 MHz, feeding is at one point that provides linear polarization of the EM fields. The commercial 3D EM simulation software Remcom Inc. XFdtd® 7.8.1.3 is used
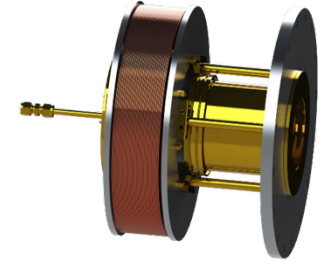


*Figure 6 IPT rendering with external electromagnet.*

to evaluate the resonance spectrum and corresponding impedances to design the antenna. The IPT structure is made of brass to minimize Eddie currents due to the RF fields, and to minimize interactions with the magnetic field. The birdcage antenna is enclosed within a brass RF shield that isolate the outer environment from the EM fields created by the antenna. The dimensions have been such to allow mounting on standard ISO-K flanges therefore minimizing the in-house required parts and enabling testing on standard facilities. XFdtd is used to evaluate the resonance frequency spectrum. Frequency is swept as signal to the antenna, and impedance $Z$ and scattering parameter $S_{11}$ over frequency are plotted. The $S_{11}$ parameter is defined as the input port voltage reflection coefficient. It represents how much power is absorbed and reflected by a load depending on the input at the signal source. Examples of the resonance study are shown for $S_{11}$ and for Z in Figure 8 and Figure 9 as exemplary result (not final) of the output from XFdtd. Each peak of $S_{11}$ is a resonant frequency, correspondingly the reactance goes to 0 at that same frequency. Indeed, there are $N/2=4$ resonance modes plus the AR one at the highest frequency. To verify that the k=1 is the correct one, the EM fields are plotted, see For further verification of the resonance frequency to be the correct one, the 3D visualization of transversal electric and magnetic fields is extracted, and compared to that of the other peaks. An example of the correct resonance with a linearly polarized field is shown in Figure 10 (top) for the magnetic field and in Figure 10 (bottom) for the electric field [17]. At each RF cycle the EM fields reverse their direction. Once the correct resonance peak is identified, the capacitance is swept until the peak is at 40.68 MHz. The externally applied magnetic field is expected to aid the formation of helicon waves within the discharge channel therefore providing a high degree of ionization [15], [24].
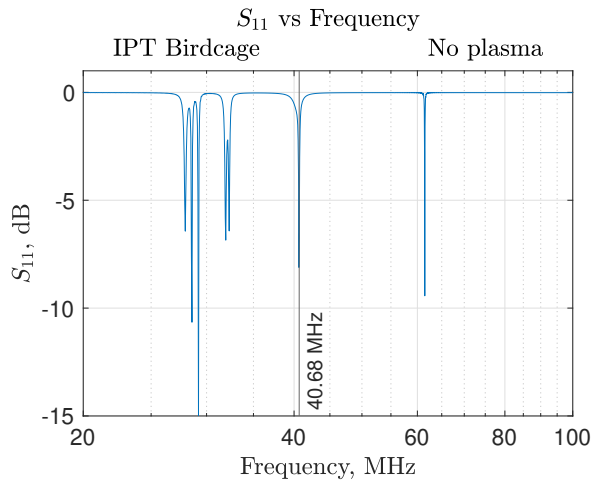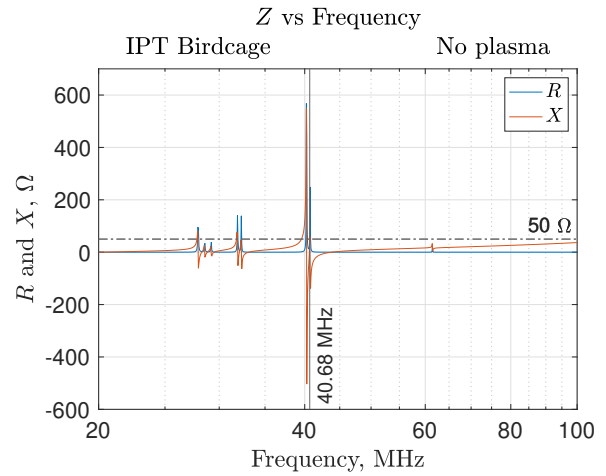
IAC-19

Figure 9 S11 vs frequency IPT



Figure 7 Z vs frequency IPT

## RESONANCE TUNING

The design for resonance ensures that it is maintained without plasma. After ignition a frequency shift and a corresponding impedance change will happen. This requires tuning, to be back at the original condition. This effect is already seen and solved in MRI machines, caused by the introduction of parts of bodies within the antenna [25], [26]. Tuning can be realized, by moving conducting components that change $X_C$ and $X_L$. This is implemented in the IPT by the moving injector, and/or by changing position and strength of the DC magnetic field. The assembled IPT is shown in Figure 11. After resonance verification, ignition is expected by the end of 2019.
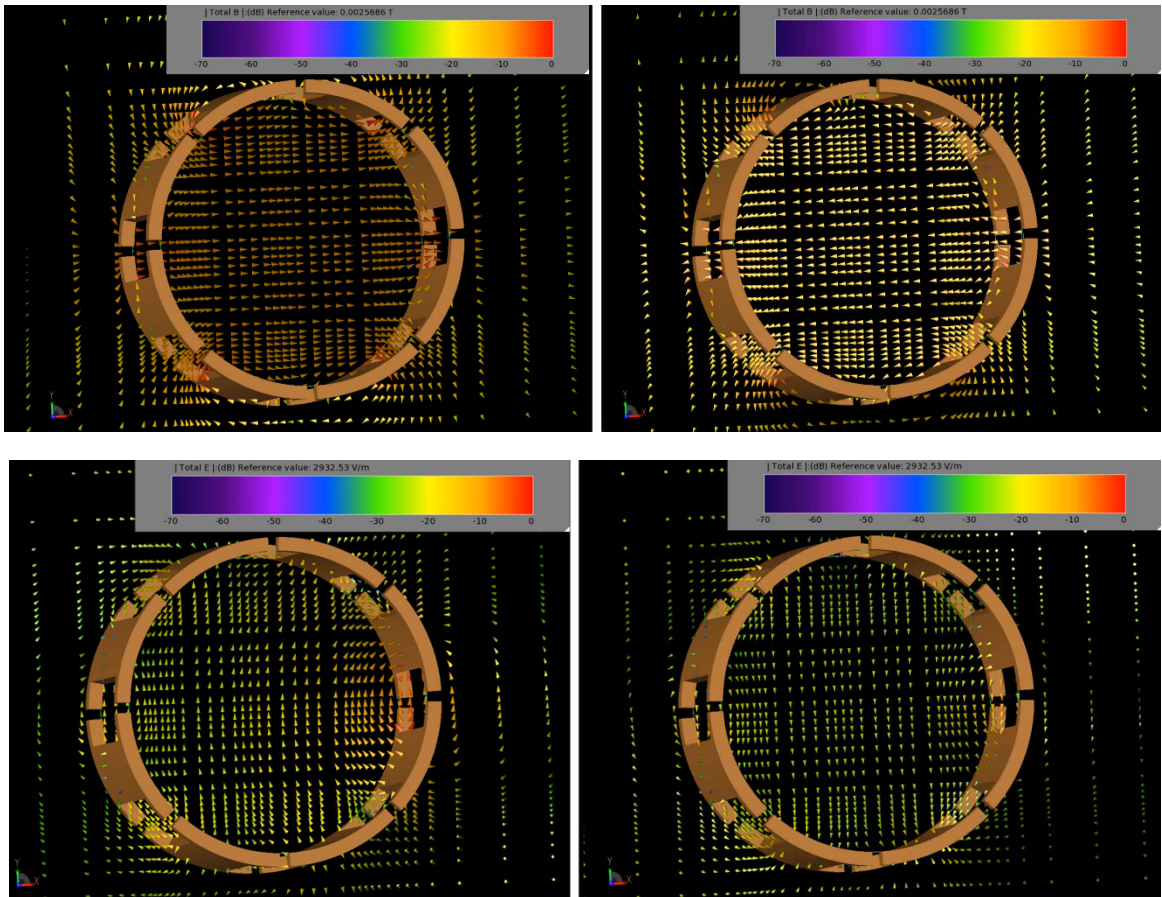


Figure 10 Magnetic Field (above) and Electric Field (below): linear polarization [17].
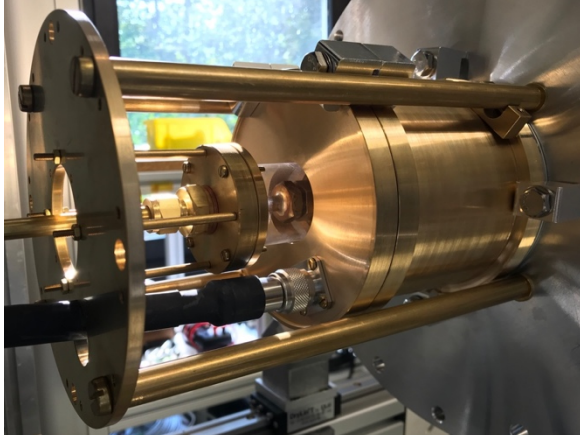
*Figure 11 IPT assembled, [17].*

## CONCLUSION

The IPT based on birdcage antenna has been designed and in the final assembly phase. The birdcage antenna operating at resonance ensure a partially matched load by having *X=0*. Moreover, the EM fields configuration produces a drift of ions and electrons towards the same direction providing partial thruster and realizing a neutral plasma plume that does not require a neutralizer. The movable injector can be used for tuning the resonance frequency, as well as the variable DC magnetic field. By the end of 2019 the IPT will be completely assembled and its resonance frequency verified. First ignition will be followed by discharge characterization for different gases and flows, powers, and magnetic field strengths. In the next years, the plasma will be evaluated by plasma diagnostic such as Langmuir and Faraday probes at first, Retarding Potential Analyser and optical emission spectroscopy as next. Further optimization of the magnetic field configuration is on going to optimize the IPT of thrust generation.

## ACKNOWLEDGEMENTS

## Bibliography

[1]     F. Romano, B. Massuti-Ballester, T. Binder, G. Herdrich, S. Fasoulas, and T. Schönherr, "System analysis and test-bed for an atmosphere-breathing electric propulsion system using an inductive plasma thruster," *Acta Astronaut.*, vol. 147, pp. 114–126, 2018.

[2]     F. Romano, B. Massuti-Ballester, T. Binder, G. Herdrich, S. Fasoulas, and T. Schönherr, "System analysis and test-bed for an atmosphere-breathing electric propulsion system using an inductive plasma thruster," *Acta Astronaut.*, vol. 147, no. October, pp. 114–126, 2018.

[3]     F. Romano, G. Herdrich, S. Fasoulas, and T. Schönherr, "Performance Evaluation of a Novel Inductive Atmosphere-Breathing EP System," *35th Int. Electr. Propuls. Conf. Atlanta, USA*, vol. IEPC-2017, no. 184, 2017.

[4]     S. Masillo *et al.*, "Analysis of electrodeless plasma source enhancement by an externally applied magnetic field for an inductive plasma thruster ( IPT ).," pp. 3–4.

[5]     M. Andrenucci, D. Feili, G. Cifali, D. Valentian, T. Misuri, and P. Rossetti, "Preliminary characterization test of HET and RIT with Nitrogen and Oxygen," no. August, pp. 1–16, 2012.

[6]     G. Cifali *et al.*, "Completion of HET and RIT characterization with atmospheric propellants," in *Space Propulsion 2012 2355386*, 2012, no. May, pp. 7–10.

[7]     T. Andreussi *et al.*, "Development and Experimental Validation of a Hall Effect Thruster RAM-EP Concept," in *35th International Electric Propulsion Conference*.

[8]     T. Andreussi *et al.*, "Development Status and Way Forward of SITAEL ' s Air-breathing Electric Propulsion," in *AIAA Propulsion and Energy Forum*, 2019, no. August.

[9]     F. Romano, G. Herdrich, P.C.E. Roberts, and et al., "Advances on the Inductive Plasma Thruster Design for an Atmosphere-Breathing EP System," *69th Int. Astronaut. Congr. Adelaide, Aust.*, no. IAC-18.C4.6.4x46387, 2018.

[10]    Romano et al, "System Analysis and Test-Bed for an Atmosphere-Breathing Electric Propulsion System Using an Inductive Plasma Thruster," *67th Int. Astronaut. Congr.*, no. September, pp. 25–29, 2017.

[11]    F. Romano, G. Herdrich, and S. Fasoulas, "Performance Evaluation of a Novel Inductive Atmosphere-Breathing EP system," in *International Electric Propulsion Conference*, 2017, no. October, pp. 1–2.

[12]    F. F. Chen and D. Arnush, "Generalized theory of helicon waves. I. Normal modes," *Phys. Plasmas*, vol. 4, no. 9, pp. 3411–3421, 1997.

[13]    D. Arnush and F. F. Chen, "Generalized theory of helicon waves. II. Excitation and absorption," *Phys. Plasmas*, vol. 5, no. 5, pp.

1239–1254, 1998.

[14] D. Melazzi and V. Lancellotti, "ADAMANT: A surface and volume integral-equation solver for the analysis and design of helicon plasma sources," *Comput. Phys. Commun.*, vol. 185, no. 7, pp. 1914–1925, 2014.

[15] F. F. Chen, "Permanent Magnet Helicon Source for Ion Propulsion," *IEEE Trans. Plasma Sci.*, vol. 36, no. 5, pp. 2095–2110, 2008.

[16] A. W. Kieckhafer and M. L. R. Walker, "Rf power system for thrust measurements of a helicon plasma source," *Rev. Sci. Instrum.*, vol. 81, no. 7, pp. 1–8, 2010.

[17] F. Romano *et al.*, "Inductive Plasma Thruster (IPT) for an Atmosphere- Breathing Electric Propulsion System: Design and Set in Operation," in *International Electric Propulsion Conference*, 2019.

[18] C. E. Hayes, W. A. Edelstein, J. F. Schenck, O. M. Mueller, and M. Eash, "An efficient, highly homogeneous radiofrequency coil for whole-body NMR imaging at 1.5 T," *J. Magn. Reson.*, vol. 63, no. 3, pp. 622–628, 1985.

[19] J. Jin, "Electromagnetics in Magnetic Resonance Imaging - IEEE Antennas and Propagation Magazine," *Clin. Imaging*, vol. 40, no. 6, pp. 7–22, 1998.

[20] A. A. Howling, P. Guittienne, C. Hollenstein, and I. Furno, "Resonant rf network antennas for inductively-coupled plasma sources."

[21] I. Furno *et al.*, "A novel helicon plasma source for negative ion beams for fusion," *Nibs*, no. September, 2016.

[22] I. Furno *et al.*, "Helicon wave-generated plasmas for negative ion beams for fusion," *EPJ Web Conf.*, vol. 157, p. 03014, 2017.

[23] P. Guittienne, E. Chevalier, and C. Hollenstein, "Towards an optimal antenna for helicon waves excitation," *J. Appl. Phys.*, vol. 98, no. 8, 2005.

[24] R. Jacquier *et al.*, "First B-dot measurements in the RAID device, an alternative negative ion source for DEMO neutral beams," *Fusion Eng. Des.*, vol. 146, pp. 1140–1144, Sep. 2019.

[25] C. E. Hayes, "The development of the birdcage resonator: A historical perspective," *NMR Biomed.*, vol. 22, no. 9, pp. 908–918, 2009.

[26] A. C. Özen, *Novel MRI Technologies for Structural and Functional Imaging of Tissues with Ultra-short $T_2$ Values*, vol. 34. KIT Scientific Publishing, 2017.